J. Biomechanics Vol. 23, No. 10, pp. 991–1000, 1990.
Printed in Great Britain

0021-9290/90 $3.00 + .00

TRENDS OF MECHANICAL CONSEQUENCES AND MODELING OF A FIBROUS MEMBRANE AROUND FEMORAL HIP PROSTHESES

H. WEINANS,* R. HUISKES* and H. J. GROOTENBOER†

* Biomechanics Section, Institute of Orthopaedics, University of Nijmegen, P.O. Box 9101, 6500 HB Nijmegen, The Netherlands and † University of Twente, Enschede, The Netherlands

Abstract—In the present study, the effects of a fibrous membrane between cement and bone in a femoral total hip replacement were investigated. The study involved the problem of modeling this fibrous membrane in finite-element analyses, and its global consequences for the load-transfer mechanism and its resulting stress patterns. A finite-element model was developed, suitable to describe nonlinear contact conditions in combination with nonlinear material properties of the fibrous membrane. The fibrous tissue layer was described as a highly compliant material with little resistance against tension and shear. The analysis showed that the load transfer mechanism from stem to bone changes drastically when such a membrane is present. These effects are predominantly caused by tensile loosening and slip at the interface, and are enhanced by the nonlinear membrane characteristics.

Using parametric analysis, it was shown that these effects on the load-transfer mechanism cannot be described satisfactorily with linear elastic models.

Most importantly, the fibrous tissue interposition causes excessive stress concentrations in bone and cement, and relatively high relative displacements between these materials.

INTRODUCTION

The formation of a soft fibrous membrane at the interface between bone and cement is a common long-term problem following total hip arthroplasty (THA). This soft interface layer can sometimes increase progressively in time, and eventually cause a clinical failure of the prosthetic fixation. Possible indications for this can be pain on weight-bearing, extensive radiolucent zones at the bone–cement interface on radiographs, and subsidence of the implant (Gruen *et al.*, 1979; Stauffer, 1982; Mjöberg *et al.*, 1985; Brand *et al.*, 1986). Several attempts have been made to study the mechanical effects of a soft layer between bone and prosthesis. Markolf *et al.* (1980) investigated the effects of a silastic liner between cement and bone in an experiment with cemented prostheses, using femur specimens. The subsidence measured upon loading was about two to twenty times higher than that associated with cemented prostheses without a silastic layer. They also found that the cement had cracked in one specimen at a relatively low load, suggesting that the soft layer resulted in higher cement stresses. In an experimental study with strain gauges, using a THA model which incorporated a thin flexible layer between cement and bone, Wright *et al.* (1985) found that the stress distributions in bone and stem were drastically changed relative to a configuration with a direct cement/bone bond.

Received in final form 28 *February* 1990.
Presented in part at the ASME Biomechanics Symposium, Cincinnati, Ohio, U.S.A., 14–17 June 1987, and at the 34th Annual Meeting of the Orthopaedic Research Society, Atlanta, Georgia, U.S.A., 1–4 February 1988.

The Finite Element Method (FEM) is used frequently for analyses of load-transfer and stress patterns in bone/prosthesis structures, to assess the adequacy of prosthetic designs (Huiskes and Chao, 1983). The FEM models applied usually assume complete interface bonding and are therefore descriptive of idealized, immediate post-operative configurations. The purpose of the present study was to develop a nonlinear FEM model accounting for soft-tissue membranes and to analyze its global effects on the load transfer from stem to bone, on the resulting stress patterns, and on the relative motions between cement and bone.

Although the histo-morphology of the fibrous tissue interface is reasonably well documented (Draenert, 1981; Goldring *et al.*, 1983; Eftekar *et al.*, 1985), relatively little is known about its mechanical properties. Hori (1981), and Hori and Lewis (1982) characterized the interface material as a parallel-fibered collagen tissue, with the fibers randomly distributed in sheets. They suggested that such a structure resists compression normal to the plane of the sheets, but transfers little shear stresses, as the sheets tend to slide over each other. In compression the membrane proved to be relatively compliant, highly nonlinear and visco-elastic. Ling (1986) also suggested that the resistance of the layer against tension and shear is very low. Hence, the following conditions will govern the mechanical characteristics of a fibrous tissue interface connection:

(1) low initial stiffness in compression;

(2) nonlinear force–deflection characteristics (material nonlinearity);

(3) negligible tensile force transmission (tensile loosening);

(4) negligible shear force transmission (slip);
(5) time dependence (visco-elastic).

The consequences of the first effect were analyzed previously by Brown *et al.* (1988) in a linear three-dimensional FEM model of the cemented femoral THA. Huiskes and Schouten (1980), Hampton (1981) and Klever (1984) studied the third and the fourth effects for the stem/cement interface, using two-dimensional and axisymmetric FEM models. Hori *et al.* (1982) and Vanderby *et al.* (1985) studied a combination of the first, second and fifth effects in a FEM model of tibial plateau fixation, using an interface profile of sinusoidal geometry and a thickness of 0.5 mm. The interface tissue was described with non-linear biphasic elements.

In the present analysis, a nonlinear two-dimensional FEM model, using quasi three-dimensional structural characteristics of the femoral THA was used to study the global consequences of the effects (1)–(4) on the load-transfer mechanism and the stress patterns, and on the relative motions between cement and bone. In contrast with a linear, fully bonded configuration, this model can be considered as a generalized description of femoral stem components surrounded by fibrous tissue in a worst-case situation.

METHODS

A two-dimensional FEM model of the femoral THA was constructed. The front plate of this model is shown in Fig. 1. In order to account for the three-dimensional structural integrity of the bone, a side plate was used, superimposed over the front plate. The non-uniform thickness pattern of the bone elements was based on an earlier analysis (Huiskes *et al.*, 1981). This modeling approach gives a reasonably accurate description of stress patterns in the frontal plane for the case of symmetric loading (Huiskes, 1980; Hampton, 1981; Huiskes *et al.*, 1986). The geometry of the prosthesis was based on the Precision Hip (Howmedica Inc., Rutherford, NJ, U.S.A.), analyzed previously by Huiskes (1990). The Finite Element mesh consists of 581 isoparametric, four-node, plane-stress elements. The orientation of the hip-joint force (up to 3000 N) and the support of the structure is indicated in Fig. 1. Table 1 shows the material properties of the different components (Huiskes, 1980). The FEM code MARC was used for the calculations (MARC Analysis Corporation, Palo Alto, CA, U.S.A.).

This model was extended with a fibrous tissue layer along the full medial and lateral cement/bone interfaces, whereby 1 mm of bone was removed. Because of the relatively small thickness of the layer, and the potential problems with small element aspect ratios, an alternative modeling approach for the interface layer was introduced by assuming force/displacement relations in normal and tangential directions of neighboring nodes on either side of the interface (Fig. 2). The effect of this description is that the normal stresses (σ_n) and the shear stresses (σ_{np}) across the layer

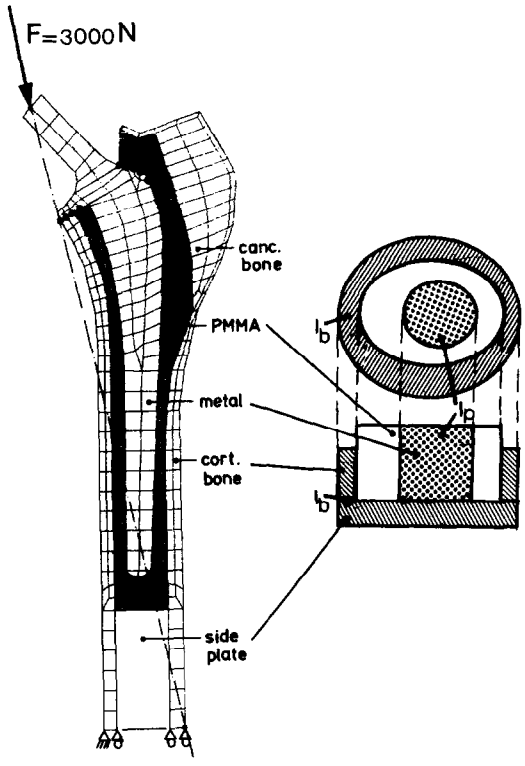

Fig. 1. The front plate of the original mesh (left) without interface layer. The elements of the front plate are of non-uniform thickness and were determined in such a way that the moments of inertia of the cortical bone and the stem (I_b and I_p) in the FE-mesh were equal to the real structure, as shown on the right. The cortical bone outside the medial lateral plane is modeled by a side plate. The circled lateral nodal points are unconnected in all cases, the medial ones only if no collar/calcar contact is assumed.

are uniform, and the parallel (bending) stress (σ_p) in the interface layer is neglected.

In order to investigate the consequences of modeling assumptions on the load-transfer mechanism, several different kinds of interface conditions were used. In the case of a *linear elastic* interface material, assuming a uniaxial strain state, the normal (ε_n) and shear (ε_{np}) strains across the layer are related to the stresses by

$$\sigma_n = \frac{E_l(1-\mu_l)}{(1+\mu_l)(1-2\mu_l)}\varepsilon_n, \tag{1}$$

$$\sigma_{np} = \frac{E_l}{2(1+\mu_l)}\varepsilon_{np}, \tag{2}$$

where E_l and μ_l are the Young's modulus and Poisson's ratio of the layer, respectively. The equations (1) and (2) were transformed in force/displacement relations between node pairs in both the directions n and p in the FEM model, Fig. 2. The forces F_n and F_p act on a surface A (Fig. 2), hence stresses in the interface layer can be expressed by $\sigma_n = F_n/A$ and $\sigma_{np} = F_p/A$. The relative displacements $\Delta U_n = U_{nb} - U_{nc}$ and $\Delta U_p = U_{pb} - U_{pc}$

Table 1. Values for the elastic moduli used in the models

Material	Elastic modulus (E) MPa
Cancellous bone	1.0×10^3
PMMA (cement)	2.0×10^3
Metal (prosthesis)	2.0×10^5
Cortical bone	1.7×10^4
Metaphyseal cortex	0.5×10^4
Side plate	1.7×10^4

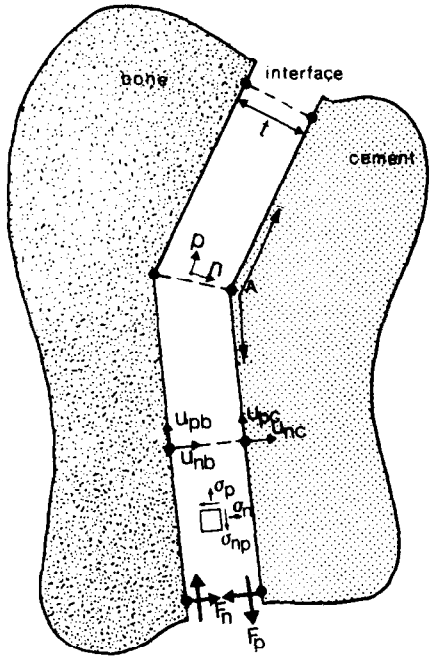

Fig. 2. Interface layer in which we indicated the directions n and p, which are always the normal and tangential directions at the corresponding nodes, the interface stresses σ_n, σ_p and σ_{np}, the interface thickness t, the reaction forces from interface material to bone and cement, and the surface A associated with the nearest node.

(Fig. 2) are related to the strain in the intermediate layer by $\varepsilon_n=\Delta U_n/t$ and $\varepsilon_{np}=\Delta U_p/t$, where t is the thickness of the layer. Hence, the equations (1) and (2) can be transformed in force–displacement relations

$$F_n=\frac{AS}{t}\Delta U_n, \tag{3}$$

$$F_p=\frac{AG}{t}\Delta U_p, \tag{4}$$

where

$$S=\frac{E_l(1-\mu_l)}{(1+\mu_l)(1-2\mu_l)} \quad \text{and} \quad G=\frac{E_l}{2(1+\mu_l)}.$$

This method is suitable to model a relatively thin linear elastic intermediate layer only. If the layer increases in thickness, the bending moment created by the longitudinal forces can no longer be neglected.

In the case of *nonlinear bonding* characteristics, tensile loosening and slip were modeled in a Newton–Raphson iterative procedure by reducing the stiffness to zero when tension or shear occurred. *Nonlinear* elastic material behavior of the fibrous membrane was described by the relations

$$\sigma_n=\frac{S_0}{\alpha}\left\{\frac{1}{(1-\varepsilon_n)^\alpha}-1\right\}, \quad \text{if } \varepsilon_n\leqslant 0 \tag{5a}$$

$$\sigma_n=0, \quad \text{if } \varepsilon_n>0 \tag{5b}$$

$$\sigma_{np}=0, \tag{5c}$$

which is in qualitative agreement with the findings of Hori and Lewis (1982). The stiffness of this material in compression is found from

$$\frac{d\sigma_n}{d\varepsilon_n}=S_0\left\{\frac{1}{(1-\varepsilon_n)^{\alpha+1}}\right\}, \tag{6}$$

hence S_0 (MPa) can be considered as the initial stiffness parameter [comparable with S in equation (3)], and α as a strain hardening factor (Fig. 3). By varying S_0 and α, the effects of the constitutive properties of the fibrous membrane in the model were studied.

Substituting the relations $\sigma_n=F_n/A$ and $\varepsilon_n=\Delta U_n/t$, equation (5a) is transformed and gives

$$F_n=\frac{S_0A}{\alpha}\left[\left(\frac{t}{t-\Delta U_n}\right)^\alpha-1\right], \tag{7}$$

from which the tangent stiffness $dF_n/d\Delta U_n$ in the model can be directly determined in each iteration of the Newton–Raphson process.

The principles of the Newton–Raphson procedure as used here are illustrated in Fig. 4 for a loadstep $\Delta F=F_2-F_1$. In this illustration the iterative process searches for the equilibrium displacement related to the force F_2. As is evident from this figure, the loadstep

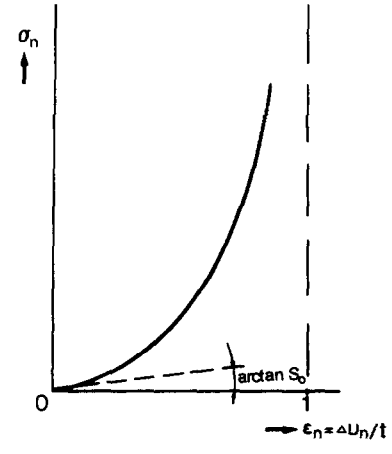

Fig. 3. Nonlinear stress–strain relation of the interface layer under compression.

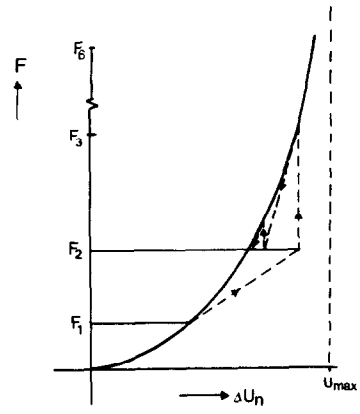

Fig. 4. The Newton–Raphson iteration process. The load-steps $F_2 - F_1$ must be applied carefully to prevent the relative displacement ΔU_n in the first iteration becoming larger than U_{max}.

must be chosen adequately in order not to exceed the asymptotic displacement value. The convergence criterion used was set to 5% of the applied force.

Because the investigation of modeling options for the fibrous interface in general and the effects of its individual characteristics were considered of interest, several models were used subsequently, each time refining the interface descriptions, and their effects compared. The models, denoted (i)–(vi), are briefly summarized in Table 2, and their associated interface force/displacement characteristics to match are identified in Fig. 5.

A conventional, linear bonded model (i) without intermediate layer was used as a reference, to test the interface description used in the subsequent models. In this model, as in the subsequent ones with the exception of model (vi), the prosthetic collar was assumed not to be in contact with the bone of the calcar.

Table 2. Characteristics of the various models investigated

Model nr.	Type of model	Thickness (t) of interface (mm)	Layer material characteristics		α	Interface connection	Collar/calcar contact
			G (MPa)	S or S_0 (MPa)			
i	Linear	0	—	—	—	Bonded	No
ii(a)	Linear	1	6538	17,000	—	Bonded	No
(b)	Linear	1	65.4	170	—	Bonded	No
(c)	Linear	1	3.8	10	—	Bonded	No
iii	Nonlinear	0.01	0	10^7	4	Loose	No
iv	Nonlinear	1	0	10	—	Loose	No
v(a)	Nonlinear	1	0	10	4	Loose	No
(b)	Nonlinear	1	0	0.17	4	Loose	No
(c)	Nonlinear	1	0	10	2	Loose	No
vi	Nonlinear	1	0	10	2	Loose	Yes

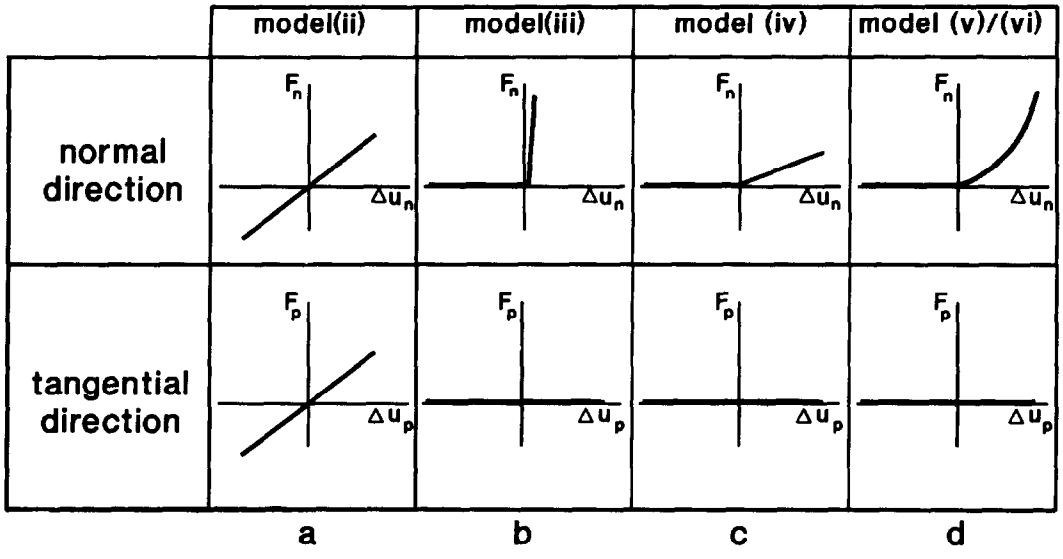

Fig. 5. The force–displacement relations as chosen in the different models: (a) model (ii), fully bonded linear elastic models; (b) model (iii), nonlinear contact model without friction, so only normal compressive forces are transferred; (c) model (iv), nonlinear contact model without friction, with a linear elastic membrane of 1 mm; (d) models (v) and (vi), nonlinear contact without friction, with a nonlinear elastic membrane.

Model (ii) features a 1 mm thick, linear elastic interface membrane [Fig. 5(a)], as described by equations (3) and (4), using stiffness values of 17,000 [ii(a)], 170 [ii(b)] and 10 MPa [ii(c)]. Model [ii(a)] was analyzed to test the interface model using the force/displacement description of opposite interface nodes, relative to the conventional description (i). The second and third analyses [ii(b)] and [ii(c)] were used to test a linear modeling approach, assuming the interface layer to be soft, but linear elastic and bonded to cement and bone, as was done previously by Brown *et al.* (1988).

Model (iii) was applied to evaluate the effects of tensile separation and slip between bone and cement, without fibrous material at the interface. Hence this represents a loose interface across which normal forces are transmitted only when the surfaces are in contact. This was achieved by choosing the stiffness between two contact points in the tangential direction as zero and in the normal direction as zero in tension and relatively high in compression [Fig. 5(b)]. In every iteration, the relative displacements (ΔU_n) in the normal direction between two contact points were calculated. The stiffness in the normal direction was given the value of zero when $\Delta U_n > 0$, which implies no contact, and a layer stiffness of 10^5 MPa when $\Delta U_n < 0$, which simulates rigid bonding. The layer stiffness cannot be taken too high in this case because the singularity ratio of the stiffness matrix can then become too small, which leads to numerical problems. The results of this model (iii) were also compared with those of an analysis using the normal gap-element of the MARC FE-code. This gap-element is based on the imposition of a gap-closure constraint and a Lagrange multiplier, representing the normal force.

In model (iv) the tensile loosening and slip characteristics described above were combined with a soft (linear) elastic interface layer, thus combining the features of models [ii(c)] and (iii), in such a way that the interface stiffnesses were taken as zero for tension and shear, and according to equation (3) in compression [Fig. 5(c)].

Model (v) was similar to model (iv), but this time the nonlinear material properties of the fibrous material were included, according to equations (5) and (6), as shown in Fig. 5(d). Three analyses were carried out with this model, whereby S_0 and α were varied according to (a) $S_0 = 10.0$ MPa, $\alpha = 4$; (b) $S_0 = 0.17$ MPa, $\alpha = 4$; and (c) $S_0 = 10.0$ MPa, $\alpha = 2$.

Finally, model (vi) was used to study the effects of collar/calcar contact in a loose prosthesis. In this case, the same interface characteristics as in model (v) were used and the collar was assumed to press frictionless on the calcar. In fact, the same interface description as in model (v) was used here also for the collar/calcar contact, assuming an interface thickness of 0.01 mm between collar and calcar. This results in a frictionless contact without tensile stresses.

The load of 3000 N was prescribed in six steps. Convergence in the nonlinear models was usually achieved after four or five iterations in the Newton–Raphson procedure (Fig. 4).

RESULTS

Linear models

The stress patterns obtained with model [ii(a)], featuring a linear elastic layer with an elastic modulus equal to bone, were virtually equal to those of the conventional model (i), indicating that the interface description using force/displacement relationships is accurate.

The effects of a reduced layer flexibility studied in the linear elastic models [ii(a)–(c)] were similar to those reported by Brown *et al.* (1988) from their (linear elastic) three-dimensional model: load-transfer stresses in the cement and at the interfaces tend to become more uniformly distributed when the layer module is reduced (Fig. 6), and the (bending) stresses in stem and bone increase somewhat [Fig. 7, [ii(c)] vs (i)]. In these linear elastic models, small displacements are assumed. In the analysis of model [ii(c)], featuring an elastic modules of 10 MPa for the layer material, a maximal strain value of 24 % was found across the layer. This result violates the above assumption, which already indicates the non-validity of a linear elastic approach.

Nonlinear bonding

The stress patterns found with model (iii), featuring nonlinear bonding characteristics (slip and tensile separation) and no intermediate layer, were equal to those obtained with a similar analysis in which the normal (frictionless) gap elements of the MARC FEM-code were used, instead of the interface–node

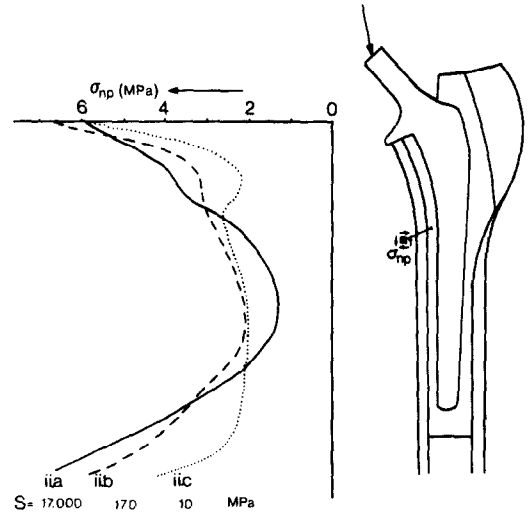

Fig. 6. Shear stresses (σ_{np}) in cement at the medial bone/cement interface for the linear fully bonded model with 1 mm interface layer, model (ii), as determined for three values of the stiffness: —— model [ii(a)], $S = 17000$ MPa; -- model [ii(b)], $S = 170$ MPa; . . . . . model [ii(c)], $S = 10$ MPa.

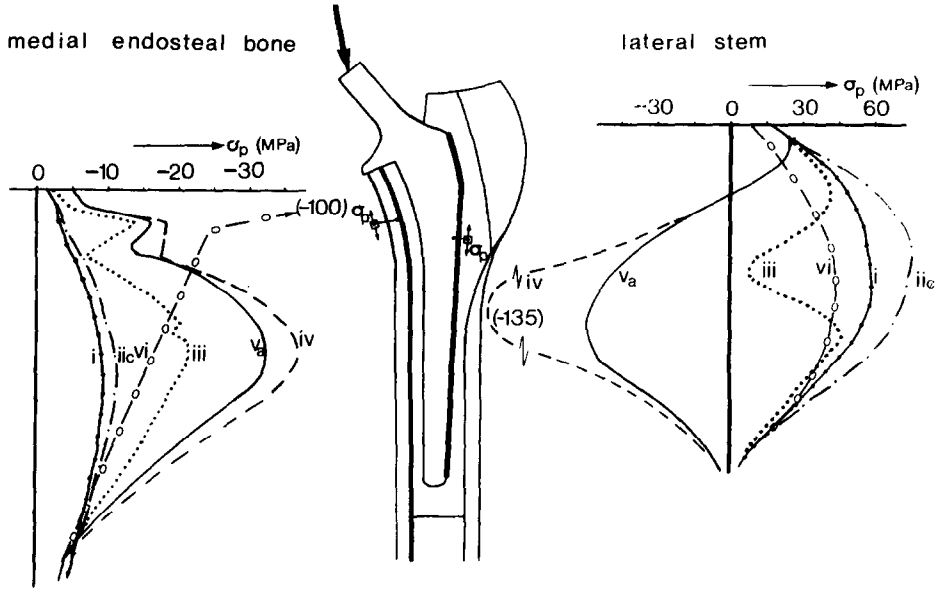

Fig. 7. Parallel (bending) stresses (σ_p) at the medial endosteal bone surface and at the lateral stem side as found in models (i)–(vi). -●-●-●- model (i), linear fully bonded conventional analysis which is equal to model [ii(a)]; -●-●-●- model [ii(a)], linear fully bonded model with 1 mm interface and $S = 17000$ MPa; –·– model [ii(c)], linear fully bonded analysis with 1 mm interface layer and $S = 10$ MPa; . . . . model (iii), nonlinear contact conditions and no interface layer; – – model (iv), nonlinear contact conditions and 1 mm linear interface layer, $S = 10$ MPa; —— model [v(a)], nonlinear contact conditions with 1 mm nonlinear interface layer, $S_0 = 10$ MPa, $\alpha = 4$; –o– model (vi), nonlinear contact conditions with 1 mm nonlinear interface layer ($S_0 = 10$ MPa, $\alpha = 4$) and collar/calcar contact.

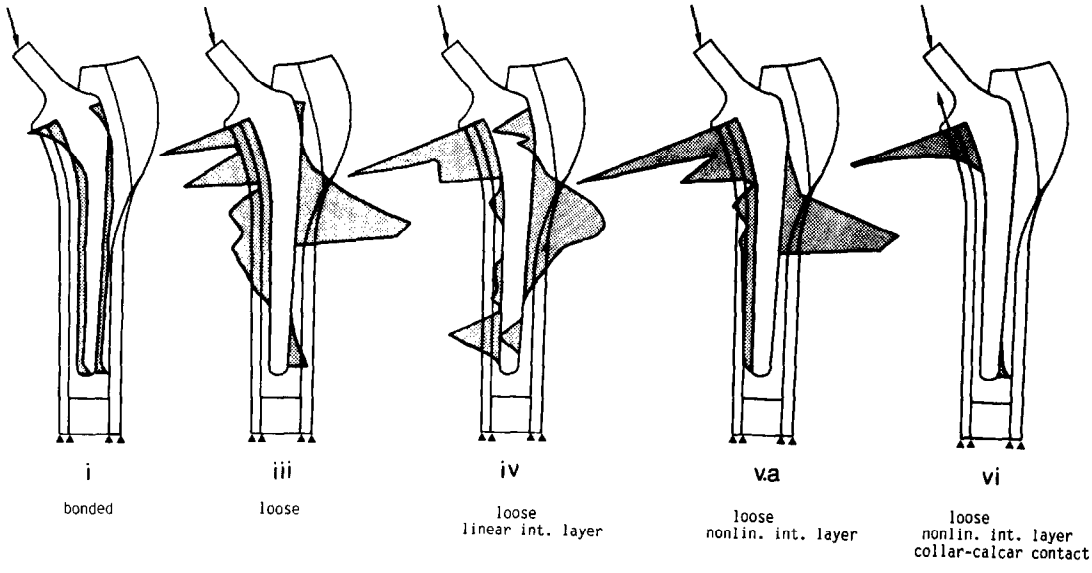

Fig. 8. Normal stresses (σ_n) in cement at the stem/cement interface, as determined for models (i)–(vi).

relationships described above, again indicating the accuracy of this modeling approach.

Relative to the bonded interface characteristics, slip and tensile separation have dramatic effects, illustrated in Figs 7 and 8. Cortical (bending) stress patterns change drastically, in fact reducing in the mid-stem region (Fig. 7). This mechanism is caused by subsidence of the prosthesis/cement complex, whereby the interface conformity between cement and bone is lost, and high compressive stress concentrations are generated at the medial/proximal and mid/lateral regions in particular [Fig. 8, (iii) vs (i)]. The stem is

thereby almost loaded as in three-point bending, as illustrated schematically in Fig. 9, which explains the reduction of tensile (bending) stress in the mid-lateral stem region in Fig. 7 [(iii) vs (i)].

This mechanism is further enhanced when the nonlinear bonding characteristics are combined with an intermediate layer with a low elastic module of 10 MPa, simulating a fibrous tissue with linear elastic properties. The bone (bending) stresses again increase more than twofold relative to model (iii), and the lateral-stem (bending) stresses even change sign from tensile to compressive (Fig. 7). This indicates that the three-point bending mechanism (Fig. 9) is enhanced in this case [Fig. 8, (iv) vs (iii)].

Although the interface bonding characteristics are nonlinear in this model, the fibrous layer is assumed to be linear elastic, which again presumes that displacements are small. In this case the maximal compressive strain across the layer was found to be 120 %, indicating penetration of cement in bone. Hence also in this case the linear elastic assumptions are violated.

Nonlinear fibrous layer

When more realistic, nonlinear properties for the fibrous layer were assumed [model (v)], the basic mechanisms and trends described above remained intact (Figs 7 and 8), [v(a) vs (iv)]. The stem and bone stresses are somewhat attenuated by the nonlinear tissue characteristics (Fig. 7), but the three-point bending mechanism (Fig. 9) with high cement stress concentrations in particular areas is still apparent (Fig. 8).

The susceptibility of the stress patterns for the values of the initial stiffness S_0 and the strain-hardening factor α in the constitutive equations for the layer were studied in models [v(a)–(c)]. The effects of a change in α from 4 to 2 are hardly noticeable (model [v(a)] vs [v(c)]). A reduction of the initial stiffness S_0 from 10.0 to 0.17 MPa results in increased interface stresses, concentrated in smaller areas.

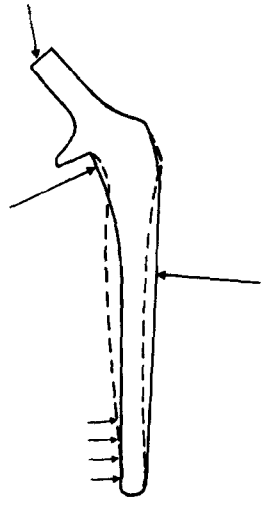

Fig. 9. Schematic illustration of the stem-deformation after loading in a three-point bending case like in models (iv) and (v).

Collar/calcar contact

When the collar is in contact with the calcar [model (vi)], the prosthesis/cement complex is prevented from subsiding, and a greater part of the axial load is transferred at the calcar. As a result, the proximal/medial bone stresses are increased and the stem stress patterns become similar to those in the linear, bonded configurations (Fig. 7). Due to the bending moment produced by the hip-joint force, the prosthesis rotates within the fibrous tissue containment, transferring load at the proximal/medial and distal/lateral regions only (Fig. 8).

Relative displacements

The relative displacements between opposite nodes at cement and bone were determined in all models. In the linear, fully bonded models, no gap or slip occurred, hence relative displacements resulted only from deformation in the interface. In Fig. 10 the relative displacements found in models (iii), (v) and (vi) are shown.

In the case of a loose interface connection only [model (iii)], a virtually uniform slip of about 0.4 mm (u_p) occurs medially and laterally, resulting in approximately the same amount of total subsidence of the cement/prosthesis complex. Relative displacement normal to the interface is virtually nonexistent in this case, indicating that gaps are extremely small. With a 1 mm fibrous layer [model (v)], the interface slip is still fairly uniform, but the values increase to about 1.5–2.5 mm, depending on the initial stiffness of the fibrous material (model [v(a)]: $S_0 = 10$ MPa; model [v(b)]: $S_0 = 0.17$ MPa). In this case the subsidence is accompanied by relative displacements between cement and bone normal to the interface, again depending on the value of S_0. If the lowest stiffness is assumed ($S_0 = 0.17$ MPa, model [v(b)]), a value of about 0.8 mm is found at the proximal/medial side, and about 0.75 mm at the mid/lateral side, indicating that the layer is almost fully compressed in these regions, which corresponds with the locations of the stress concentrations discussed earlier.

When collar/calcar contact is present [model (vi)], the slip (and hence also the subsidence), virtually diminishes. Relative displacements normal to the interface remain, however, particularly at the proximal and distal sides, indicating a pivot motion of the cement/prosthesis complex relative to the bone about a point in the mid-stem region, of about 0.8°.

Contrary to the effects of the initial stiffness S_0, a change in the strain hardening factor α from 2 to 4 for the fibrous material has only a very small effect on the behavior of the bone/prosthesis structure, as illustrated in Fig. 11, showing slip at the mid-lateral region

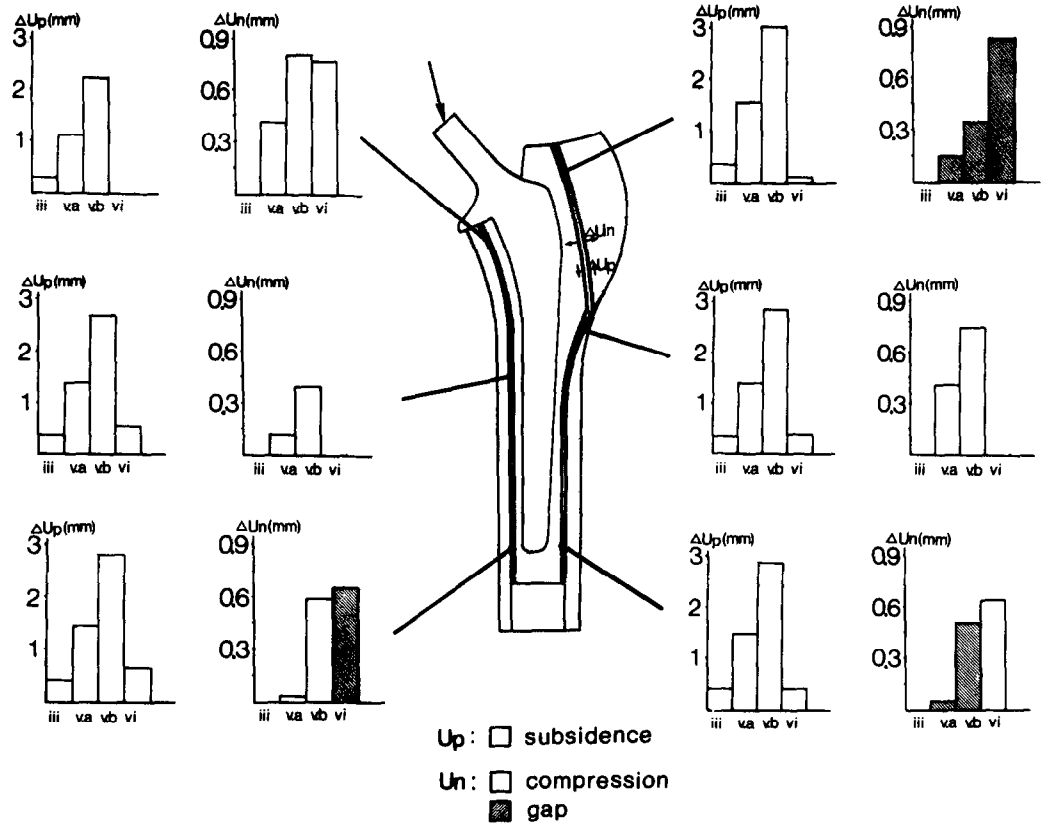

Fig. 10. Relative displacements between cement and bone in the longitudinal direction, ΔU_p (subsidence), and tangential direction, ΔU_n (compression or gap formation), for the models (iii), (v) and (vi).

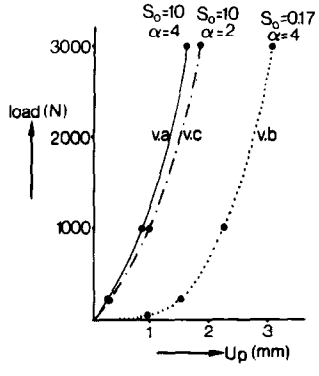

Fig. 11. Force–slip relation at the mid-lateral area for the loose model with the 1 mm nonlinear interface layer and no collar/calcar contact, model (v), as determined for different values of S_0 and α. —— model [v(a)], $S_0 = 10.0$, $\alpha = 4$; -·- model [v(b)], $S_0 = 0.17$, $\alpha = 4$; ..... model [v(c)], $S_0 = 10.0$, $\alpha = 2$.

for several values of S_0 and α, determined with model (v). Although S_0 and α affect the absolute values of relative motions and stress values, the relative patterns did not change significantly.

DISCUSSION

It must be appreciated that the models used here offer only first-order descriptions of the complex reality. The precise constitutive behavior of the loose interface, with or without a fibrous membrane, is uncertain, and a simplified two-dimensional geometry had to be adopted in view of the nonlinear character of the solution process and the requirements for extensive parametric variations. As a consequence, the results presented are merely indicative of the effects of prosthetic loosening, and are useful for the understanding of post-failure mechanisms.

The fibrous tissue layer has a very low initial stiffness relative to cement and bone, but displays strain hardening when compressed (Hori and Lewis, 1982), resulting in progressively increasing stiffness, and large strains. By assuming a stress–strain relationship as used here in the fully nonlinear model (v), the most important features of this behavior (low initial stiffness, strain hardening and large strains) can be accounted for, whereas their effects can be studied in a relatively simple fashion. The incorporation of the fibrous tissue in the FEM model by using nodal-point relationships rather than elements must also be seen as a compromise. With the present formulation, the

interrelationship between shear- and normal stress-transfer is uncoupled, there is no lateral contraction, and axial (bending) stresses in the layer are not accounted for. However, the first two factors influence mainly the parameters S_0 and α, the precise values of which are unknown anyway, and whose effects can be studied by parametric analysis. The consequence of neglecting the axial stresses is thought to be a minor one, because these stresses will be very small, due to the low stiffness of the material relative to the cement and the bone. In earlier analyses of bone/prosthesis structures, using similar beam-on-elastic-foundation formulations for the cement layer in linear models, quite reasonable results were obtained (Huiskes, 1980). In any case, a comparison of the present approach to a conventional calculation (model (i) vs model [ii(a)]) showed excellent agreement of all stress components. It must be noted, however, that this approach is only valid if the layer is relatively thin.

A second limitation of the present analysis is an effect of the choice for uniform layer thickness. It is intuitively obvious that the stress transfer across the layer would be greatly influenced by interrupted cement–bone contact, which would 'stress-shield' the soft tissue and prevent relative interface motions. A similar mechanism would occur in the case where the fibrous layer does not extend along the full cement–bone connection. Fibrous tissue morphology can differ greatly in a patient population, so the present results represent a particular configuration only, not necessarily a typical one. Vanderby *et al.* (1985), in their analysis of tibial plateau fixation with a central post in the knee joint, assumed a sinusoidal interface geometry enclosing the fibrous membrane. In this case tangential slip is locally constrained by the interface geometry in such a way that shear loads can be transferred after some subsidence has occurred.

In view of the complex, irregular geometry of the femoral bone/prosthesis structure, the two-dimensional characteristics of the FEM model present another serious limitation. The present 'side-plate' model with nonuniform element thickness quite reasonably represents the behavior of the real structure in the frontal plane, in the case that the interfaces are bonded (Huiskes, 1980; Hampton, 1981; Huiskes *et al.*, 1986). However, in the case that interfaces are loose and soft tissue is interposed, it is quite possible, in fact likely, that the asymmetry of the bone relative to the frontal plane, in combination with torsion (out-of-plane loading) would result in significant rotation and out-of-plane deformations which are not accounted for in the present model.

Finally, it must be appreciated that the present analysis is a quasi-static one in which the effects of a single force on the prosthesis, (slowly) increasing from 0 to 3000 N are investigated. In reality, the load will be multidirectional, and muscle forces will occur as well, while visco-elastic effects will influence the constitutive behavior of the fibrous material, depending on the loading rate.

In spite of the model limitations the parametric analysis gives some insight into the requirements for modeling the mechanical behavior of the loosening prosthesis. It is evident from the present results that a linear approach to this problem is inadequate, because it neglects the most important of the occurring phenomena. Although some effects are seen from assuming a thin layer with a reduced modules at the interface, similar to those reported by Brown *et al.* (1988), these do not nearly represent the effects of a fibrous membrane, assuming the low resistance of the fibrous layer against tension and shear. It was shown here to be essential to include the latter, which implies a nonlinear interface condition. Combining such a description with a linear elastic layer material [model (iv)] gives reasonable stress results in a qualitative sense, but overestimates the deformation in the layer, because its strain-hardening behavior in compression is neglected. Including this nonlinear behavior is of particular importance when relative displacements (or motions) between implant and bone are to be evaluated.

Some important conclusions relative to load transfer in prosthetic fixations can be drawn from the present analysis. The load-transfer mechanism and the associated stress patterns depend on four aspects: loading characteristics, geometry, material properties, and boundary/interface conditions. The present results show, in comparison with earlier analyses (Huiskes, 1990), that of these four the interface conditions represent by far the most important aspect. A loose cement/bone interface, allowing slip and tensile loosening, changes the load-transfer mechanism drastically, relative to a bonded interface. When a soft tissue layer is present as well, even more dramatic changes occur, resulting in very high local cement and interface stress concentrations, and a re-orientation of the loading patterns in the stem and the bone. These phenomena are due in particular to (elastic) subsidence of the cement/prosthesis complex, whereby the original conformity of the cement–bone connection is lost. In view of this mechanism, it is obvious that the actual stress patterns in a particular case would depend predominantly on the actual interface geometry, which determines where the prosthesis would find its secondary support. Hence, for a realistic actual case, the geometry should be realistically accounted for in a model in contrast to the material properties of the interface material, which seems to be of minor influence.

A collared prosthesis would prevent the subsidence of the cement/prosthesis complex, because the load is predominantly transferred between collar and calcar, which is indeed seen in the results of model (vi). As a consequence, the stress concentrations in the cement and at the interfaces are relocated and reduced and the stem and bone stress patterns correspond more with

those in the bonded models. The subsidence is translated in a pivot motion of the cement/prosthesis complex relative to the bone and a subsequent repetitive compression and release of the proximal and distal fibrous layers. According to Perren and Rahn (1980), this interface load in particular would cause bone to resorb.

The clinical significance of the present findings, finally, can only be formulated in general terms, again because interfaces and fibrous tissue layers occur in many different configurations, of which only one example was studied here. It is evident from the present results, however, that interface loosening and fibrous tissue formation dramatically change the load-transfer mechanism, resulting in high stress concentrations locally in the cement layer and the adjacent bone, and in considerable relative motions between cement and bone. It is not unlikely that local cement and bone failures will occur, which could cause rapid propagation of mechanical loosening to a clinical failure. In addition, the relative motions at the interface are likely to cause progressive bone resorption (Perren and Rahn, 1980; Goldring *et al.*, 1983; Hüiskes and Nunamaker, 1984; Strens, 1986). Hence, the present results are consistent with the hypothesis that progressive fibrous tissue formation and clinical loosening have a mechanical basis.

Acknowledgement—This project was sponsored in part by the Netherlands Organization for Research (NWO/Medigon).

REFERENCES

Brand, R. A., Pedersen, D. R. and Yoder, S. A. (1986) How definition of 'loosening' affects the incidence of loose total hip reconstructions. *Clin. Orthop.* **210**, 185–191.

Brown, T. D., Pedersen, D. R., Radin, E. L. and Rose, R. M. (1988) Global mechanical consequences of reduced cement/bone coupling rigidity in proximal femoral arthroplasty: a three-dimensional finite element analysis. *J. Biomechanics* **21**, 115–129.

Draenert, K. (1981) Histomorphology of the bone-to-cement interface: remodeling of the cortex and revascularization of the medullary canal in animal experiments. In *The Hip* (Edited by Salvati, E. A.), *Proc. 9th Mtg Hip Soc.*, pp. 71–110, CV Mosby Co., St Louis.

Eftekar, N. S., Doty, S. B., Johnston, A. D. and Parisien, M. V. (1985) Prosthetic synovitus. In *The Hip* (Edited by Fitzgerald, R. H.), *Proc. 13th Mtg Hip Soc.*, pp. 169–183. CV Mosby Co., St Louis.

Goldring, S. R., Schiller, A. L., Roelke, M., Rourke, C. M., O'Neill, D. A. and Harris, W. H. (1983) The synoviallike membrane at the bone–cement interface in loose total hip replacements and its proposed role in bone lysis. *J. Bone Jt Surg.* **65A**, 575–584.

Gruen, T. A., McNeice, G. M. and Amstutz, M. D. (1979) Modes of failure of cemented stem-type femoral components. *Clin. Orthop.* **141**, 17–27.

Hampton, S. J. (1981) A nonlinear finite element model of adhesive bond failure and application to total hip replacement analysis. Ph.D. thesis, University of Illinois at Chicago Circle.

Hori, R. Y. (1981) Investigation of the bone–prosthesis interface following total joint replacement. Ph.D. dissertation, North Western University, Chicago, Illinois.

Hori, R. Y. and Lewis, J. L. (1982) Mechanical properties of the fibrous tissue found at the bone–cement interface following total joint replacement. *J. Biomed. Mater. Res.* **16**, 911–927.

Hori, R. Y., Lewis, J. L., Hammer, R. S. and Askew, M. J. (1982) The effect of a fibrous tissue liner between bone and cement on finite element models of bone–prosthesis structures. *Trans. 28th A. Mtg Orthop. Res. Soc.*, New Orleans, Louisiana, 19–21 January, p. 146.

Huiskes, R. (1980) Some fundamental aspects of human joint replacement. *Acta orthop. scand. Suppl.* 185.

Huiskes, R. (1990) Comparative stress patterns in cemented total hip arthroplasty. In *Proc. Book Symp. Orthop. Surg. Bone Jts*, Munich, 28–29 November 1986. *Orthop. Rel. Sci.* **1**, 93–108.

Huiskes, R. and Chao, E. Y. S. (1983) A survey of finite element analysis in orthopaedic biomechanics: the first decade. *J. Biomechanics* **16**, 385–409.

Huiskes, R., Janssen, J. D. and Slooff, T. J. (1981) A detailed comparison of experimental and theoretical stress-analyses of a human femur. In *Mechanical Properties of Bone*, AMD Vol. 45, (Edited by Cowin, S. C.), pp. 211–234. The American Society of Mechanical Engineers, NY.

Huiskes, R. and Nunamaker, D. (1984) Local stresses and bone adaption around orthopaedic implants. *Calcif. Tissue Int.* **36**, S110–S117.

Huiskes, R. and Schouten, R. Y. (1980) The effect of interface loosening on the stress distribution in intramedullary fixated artifical joints. In *Advances in Bioengineering* (Edited by Mow, V. C.), pp. 213–217. The American Society of Mechanical Engineers, NY.

Huiskes, R., Snijders, H., Vroemen, W., Chao, E. Y. S. and Morrey, B. F. (1986) Fixation stability of a short cementless hip prosthesis. *Trans. 32nd A. Mtg Orthop. Res. Soc.*, New Orleans, Louisiana, 17–20 February, p. 466.

Klever, F. J. (1984) On the mechanics of failure of artificial knee joints. Ph.D. dissertation, University of Twente, The Netherlands.

Ling, R. S. M. (1986) Observation on the fixation of implants to the bone skeleton. *Clin. Orthop.* **210**, 80–96.

Markolf, K. L., Amstutz, H. C. and Hirschowitz, D. L. (1980) The effect of calcar contact on femoral component micromovement. A mechanical study. *J. Bone Jt Surg.* **62B**, 1315–1323.

Mjöberg, B., Brisman, J., Hansson, L. I., Petersson, H., Selvik, G. and Önnerfält, R. (1985) Definition of endoprosthetic loosening. *Acta orthop. scand.* **56**, 469–473.

Perren and Rahn (1980) Biomechanics of fracture healing. *Can. J. Surg.* **20**, 228–231.

Stauffer, R. N. (1982) Ten year follow-up study of total hip replacement with particular reference to roentgenographic loosening of the components. *J. Bone Jt Surg.* **64A**, 983–990.

Strens, P. H. G. E. (1986) Analysis of implant failure in the Wagner resurfacing arthroplasty. Doctoral dissertation, University of Nijmegen, The Netherlands.

Vanderby, R., Lewis, J. L. and Chapman, S. M. (1985) Biphasic modeling of fibrous tissue at the bone–prosthesis interface in total joints *Trans. Winter A. Mtg ASME*, pp. 22–23.

Wright, K. W. J., Meswania, J. M. and Scales, J. T. (1985) Load transmission characteristics of intramedullary stem/PMMS fixation in endoprosthesis following tumour resection. International symposium on Limb Solvage in musculoskeletal oncology. *Orthop. Trans.* **10**, 38.